ELSEVIER

CrossMark

IUTAM Symposium on Multiphase flows with phase change: challenges and opportunities, Hyderabad, India (December 08 – December 11, 2014)

Numerical modelling of debris bed water quenching

D. Pavlidis[a,*], J. L. M. A. Gomes[b], P. Salinas[a], C. C. Pain[a], A. A. K. Tehrani[c],
M. Moatamedi[d], P. N. Smith[a], A. V. Jones[a], O. K. Matar[e]

[a]Dept. Earth Science & Engineering, Imperial College London, London SW7 2AZ, UK
[b]School of Engineering, University of Aberdeen, Aberdeen AB24 3UE, UK
[c]Office for Nuclear Regulation, Bootle L20 7HS, UK
[d]Centre for Nuclear Engineering, Imperial College London, London SW7 2AZ, UK
[e]Dept. Chemical Engineering, Imperial College London, London SW7 2AZ, UK

Abstract

Debris beds may be formed during a nuclear reactor severe accident and coolability of these beds is important to avoid release of radioactive materials into the environment. However, debris bed water quenching is challenging to understand, and model, because of the complex multi-phase flow and heat transfer physics involved which may include boiling. This paper develops a modelling method for boiling and demonstrates its abilities with some applications. The model is based on a multi-fluid approach, in which one phase represents the liquid, the second phase the gas phase the third phase represents the solid debris bed. In each fluid phase a set of conservation equations for mass, energy and momentum are solved with appropriate inter-phase exchange terms coupling the fluid phases.

© 2015 The Authors. Published by Elsevier B.V. This is an open access article under the CC BY-NC-ND license (http://creativecommons.org/licenses/by-nc-nd/4.0/).
Peer-review under responsibility of Indian Institute of Technology, Hyderabad.

Keywords:
Boiling modelling; heat transfer; melt pool; porous media flow.

1. Introduction

In the event of prolonged loss of cooling within a nuclear reactor integrity of internal structures may be compromised and materials might melt. This will form a debris bed which consist of fragments from the cladding and pellets that constitute the nuclear fuel. If it is not rapidly cooled, this mass will begin to melt and become harder to cool.

Here a method for simulating such environments using a multi-fluid approach is presented. This includes flooding of porous media and boiling.

The remainder of this paper is organised as follows. A brief description of the model is given in section 2 and preliminary results are presented in section 4. Finally, some concluding remarks are given in section 5.

---

* Corresponding author. Tel.: +44-020-7594-9986.
  E-mail address: dimitrios.pavlidis@imperial.ac.uk

2. Model Equations for Boiling

In this section the governing multi-phase fluid equations and modelling assumptions are presented. The basic assumption is that the system can be modelled using a three-fluid model, representing the liquid, steam and solid phases, in which the debris bed is the solid phase.

2.1. Conservation of mass

The continuity equation for phase k is expressed by:

$$\frac{\partial}{\partial t}\left(\alpha_k \rho_k\right) + \nabla \cdot \left(\alpha_k \rho_k v_k\right) = \Gamma_k, \tag{1}$$

where t is the time variable, ρ_k, α_k and v_k are the density, volume fraction and velocity of phase k, respectively, and Γ is a source/sink term that accounts for mass exchange between phases.

2.2. Force balance equations

The force balance equations are expressed by:

$$\alpha_l \rho_l \left(\frac{\partial v_l}{\partial t} + v_l \cdot \nabla v_l\right) = -\alpha_l \nabla p + \nabla \cdot \tau_l + \alpha_l \rho_l g + \Sigma_{lg}\left(v_g - v_l\right) + \Sigma_{sl}\left(v_s - v_l\right), \tag{2}$$

$$\alpha_g \rho_g \left(\frac{\partial v_g}{\partial t} + v_g \cdot \nabla v_g\right) = -\alpha_g \nabla p + \nabla \cdot \tau_g + \alpha_g \rho_g g + \Sigma_{lg}\left(v_l - v_g\right) + \Sigma_{sg}\left(v_s - v_g\right) + F_{\text{VM}} + F_{\text{IP}}, \tag{3}$$

$$\alpha_s \rho_s \left(\frac{\partial v_s}{\partial t} + v_s \cdot \nabla v_s\right) = -\alpha_s \nabla p + \nabla \cdot \tau_s + \alpha_s \rho_s g + \Sigma_{sl}\left(v_l - v_s\right) + \Sigma_{sg}\left(v_g - v_s\right) - \Sigma_{ss} v_s, \tag{4}$$

where τ is the deviatoric stress tensor, the Σ's are the inter-facial drag coefficients, p is the shared pressure of all phases; g is the gravitational acceleration. Subscripts g, l and s denote the gas, liquid and solid debris bed (porous medium) phases, respectively. The absorption coefficient Σ_{ss} is used here to ensure that the solid phase remains immobile. The virtual mass and inter-phase pressure terms are given by:

$$F_{\text{VM}} = \frac{\alpha_g \rho_l}{2}\left(\frac{\partial v_l}{\partial t} + v_l \cdot \nabla v_l - \frac{\partial v_g}{\partial t} - v_g \cdot \nabla v_g\right) \text{ and } F_{\text{IP}} = \frac{1}{4}\alpha_g \rho_l \left(v_g - v_l\right)^2 \nabla \alpha_g. \tag{5}$$

2.3. Internal energy conservation

The equations for internal energy $\left(e_l, e_g, e_s\right)$ expressed in terms of temperature $\left(T_l, T_g, T_s\right)$, in non-conservative form, are:

$$C_{p_l} \rho_l \alpha_l \left(\frac{\partial T_l}{\partial t} + v_l \cdot \nabla T_l\right) = -p\left(\frac{\partial \alpha_l}{\partial t} + \nabla \cdot \alpha_l v_l\right)$$
$$+\nabla \cdot \left(\alpha_l \kappa_l \nabla T_l\right) + \Sigma_{lg}^T\left(T_g - T_l\right) + \Sigma_{sl}^T\left(T_s - T_l\right) + \Sigma_{vap_l}\left(T_{sat} - T_l\right)$$
$$+\Gamma_l h_l + \Gamma_l L_{e0} - \Gamma_l C_{p_l} T_l, \tag{6}$$

$$C_{p_g} \rho_g \alpha_g \left(\frac{\partial T_g}{\partial t} + v_g \cdot \nabla T_g\right) = -p\left(\frac{\partial \alpha_g}{\partial t} + \nabla \cdot \alpha_g v_g\right)$$
$$+\nabla \cdot \left(\alpha_g \kappa_g \nabla T_g\right) + \Sigma_{lg}^T\left(T_l - T_g\right) + \Sigma_{sg}^T\left(T_s - T_g\right) + \Sigma_{vap_g}\left(T_{sat} - T_g\right)$$
$$+\Gamma_g h_g - \Gamma_g C_{p_g} T_g, \tag{7}$$

$$C_{p_s}\rho_s\alpha_s\left(\frac{\partial T_s}{\partial t} + v_s \cdot \nabla T_s\right) = -p\left(\frac{\partial \alpha_s}{\partial t} + \nabla \cdot \alpha_s v_s\right)$$

$$+\nabla \cdot (\alpha_s\kappa_s\nabla T_s) + \Sigma_{sl}^T(T_l - T_s) + \Sigma_{sg}^T\left(T_g - T_s\right) + S_s, \tag{8}$$

where C_p, κ and h are the heat capacity, thermal conductivity and enthalpy, respectively. The Σ^T's are inter-facial heat transfer coefficients and the Σ_{vap}'s are volumetric heat transfer coefficients due to vapourisation-condensation. T_{sat} is the saturation temperature and $L_{e0} = 2.26 \times 10^6$J/kg. The source term S_s can be used to include decay heat to the model.

It is now easy to see the effect of latent heat. On summing these two equations the interface heat exchange terms disappear, due to the interface Stefan condition (see section 3.3), leaving the term $L_{e0}\Gamma_l$ acting as a sink when boiling ($\Gamma_g = -\Gamma_l > 0$) and relaxing the liquid temperature towards T_{sat}.

3. Parametrisations

In this section the parametrisations used are briefly outlined. They are primarily taken from [2,3].

3.1. Force balance equations

The inter-facial drag coefficients are:

$$\Sigma_{sg} = 150\frac{\alpha_{gs}^2\mu_g}{\alpha_{sg}d_p^2} + \frac{7}{4}\frac{\alpha_{gs}\rho_g\left|v_g - v_s\right|}{d_p}, \ \Sigma_{sl} = 150\frac{\alpha_{ls}^2\mu_l}{\alpha_{sl}d_p^2} + \frac{7}{4}\frac{\alpha_{ls}\rho_l\left|v_l - v_s\right|}{d_p}, \ \Sigma_{lg} = \frac{3}{4}C_D\frac{\alpha_{lg}\alpha_{gl}\rho_l\left|v_g - v_l\right|}{d_b}\alpha_{lg}^{-2.65}, \quad (9)$$

where d_p is the debris bed particle diameter, d_b is the average bubble diameter and the drag coefficient C_D is related to the Reynolds number Re_{lg} by:

$$C_D = \begin{cases} \frac{24}{\alpha_{lg}Re_{lg}}\left\{1 + 0.15\left(\alpha_{lg}Re_{lg}\right)^{0.687}\right\} & \text{, if } \alpha_{lg}Re_{lg} < 1000 \\ 0.44 & \text{, if } \alpha_{lg}Re_{lg} \geq 1000 \end{cases} \tag{10}$$

and:

$$Re_{lg} = \frac{\rho_l\left|v_g - v_l\right|d_b}{\mu_l}. \tag{11}$$

The average bubble diameter is calculated using:

$$d_b = \frac{\text{We}\sigma}{\rho_l\left(v_g - v_l\right)^2}, \tag{12}$$

where We = 5 and $\sigma = 0.06$N/m. The bubble size is capped according to:

$$d_b = \min\left\{d_p, \max\left\{10^{-7}, d_b\right\}\right\}. \tag{13}$$

The normalised volume fractions are given by:

$$\alpha_{sg} = \frac{\alpha_s}{\alpha_s + \alpha_g}, \ \alpha_{gs} = \frac{\alpha_g}{\alpha_s + \alpha_g}, \ \alpha_{sl} = \frac{\alpha_s}{\alpha_s + \alpha_l}, \ \alpha_{ls} = \frac{\alpha_l}{\alpha_s + \alpha_l}, \ \alpha_{lg} = \frac{\alpha_l}{\alpha_l + \alpha_g}, \ \alpha_{gl} = \frac{\alpha_g}{\alpha_l + \alpha_g}. \tag{14}$$

3.2. Heat transfer coefficients

The inter-facial heat transfer coefficients are calculated using the Ranz-Marshall correlation valid for spherical bubbles or particles:

$$Nu = \frac{hd}{\kappa} = 2 + 0.6Re^{\frac{1}{2}}Pr^{\frac{1}{3}}, \tag{15}$$

where Nu, $Re \in [0, 200]$ and $Pr \in [0, 250]$ are the dimensionless Nusselt, Reynolds and Prandtl numbers, respectively. Therefore:

$$\Sigma_{sl}^T = \frac{\kappa_l}{d_p}\left(2 + 0.6Re_{sl}^{\frac{1}{2}}Pr_l^{\frac{1}{3}}\right), \ \Sigma_{sg}^T = \frac{\kappa_g}{d_p}\left(2 + 0.6Re_{sg}^{\frac{1}{2}}Pr_g^{\frac{1}{3}}\right), \ \Sigma_{lg}^T = \frac{\kappa_l}{d_b}\left(2 + 0.6Re_{lg}^{\frac{1}{2}}Pr_l^{\frac{1}{3}}\right), \quad (16)$$

where:

$$Re_{sl} = \frac{\rho_l |v_l - v_s| d_p}{\mu_l}, \ Re_{sg} = \frac{\rho_g |v_g - v_s| d_p}{\mu_g}. \quad (17)$$

3.3. Interface Stefan condition for mass transfer from heat transfer

The interface Stefan condition for mass transfer from heat transfer is determined by considering the thermal energy equation over the interface between the liquid and vapour/gas and ignoring storage terms in the equations. The Stefan condition is parametrised here by summing the heat transfer and mass transfer terms for vapour in the energy equations and setting this balance to zero:

$$\Sigma_{vap_l}(T_{sat} - T_l) + \Sigma_{vap_g}(T_{sat} - T_g) + \Gamma_g L_h = 0, \quad (18)$$

in which we have used the latent heat L_h:

$$\Gamma_g h_g + \Gamma_l h_l = \Gamma_g(h_g - h_l) = \Gamma_g L_h, \quad (19)$$

and also $\Gamma_g = -\Gamma_l$. Thus, the mass transfer rate Γ_g is determined from:

$$\Gamma_g = -\frac{\Sigma_{vap_l}(T_{sat} - T_l) + \Sigma_{vap_g}(T_{sat} - T_g)}{L_h}, \quad (20)$$

where:

$$h_l = \begin{cases} -L_{e0} + C_{p_l}T_l + \frac{p}{\rho_l} & , \text{if } T_{sat} < T_l \\ -L_{e0} + C_{p_l}T_{sat} + \frac{p}{\rho_l} & , \text{if } T_{sat} \geq T_l, \end{cases} \quad (21)$$

$$h_g = \begin{cases} C_{p_g}T_{sat} + \frac{p}{\rho_g} & , \text{if } T_{sat} < T_g \\ C_{p_g}T_l + \frac{p}{\rho_g} & , \text{if } T_{sat} \geq T_g. \end{cases} \quad (22)$$

Based on[3], the heat transfer coefficient Σ_{vap_l} is calculated by:

$$\Sigma_{vap_l} = \begin{cases} \max\left\{\frac{\kappa_l}{d_b}\frac{12}{\pi}|T_{sat} - T_l|\frac{\rho_l C_{p_l}}{\rho_g L_h}\beta, \ \frac{\kappa_l}{d_b}\left(2 + 0.74\left(\alpha_l Re_l\right)^{0.5}\right)\right\}\frac{3.6\alpha_b}{d_b} & , \text{if } T_{sat} < T_l \\ \min\left\{\Sigma_{vap_l}^{max}, \ \frac{F_5 L_h \rho_l \alpha_g}{\rho_l - \rho_g}\right\} & , \text{if } T_{sat} \geq T_l, \end{cases} \quad (23)$$

where $\beta = 1$, $\alpha_b = \max\{\alpha_g, 10^{-5}\}$,

$$F_5 = \begin{cases} 0.075 + 1.8\varphi C \exp(-45\alpha_b) & , \text{if } \alpha_g < 0.25 \\ 0.075 & , \text{if } \alpha_g \geq 0.25, \end{cases} \quad (24)$$

$$\varphi = \begin{cases} 1 & , \text{if } |v_g - v_l| \leq 0.61\text{m/s} \\ \left(1.639344 |v_g - v_l|\right)^{0.47} & , \text{if } |v_g - v_l| > 0.61\text{m/s}, \end{cases} \quad (25)$$

$$C = \begin{cases} 65 - 5.69 \times 10^{-5}\left(p - 10^5\right) & , \text{if } p \leq 1.1272 \times 10^6\text{Pa} \\ 2.5 \times 10^9 p^{-1.418} & , \text{if } p > 1.1272 \times 10^6\text{Pa}, \end{cases} \quad (26)$$

$$\Sigma_{vap_l}^{max} = 17539 \max\left\{4.724, 472.4\alpha_g\alpha_l\right\} \max\left\{0, \min\left\{1, \frac{\alpha_g}{0.1}\right\}\right\}. \quad (27)$$

The heat transfer coefficient Σ_{vap_g} is calculated by:

$$\Sigma_{vap_g} = 10^4 \frac{3.6\alpha_b}{d_b}. \tag{28}$$

The final value of the heat transfer coefficients for the liquid and gas are limited by a maximum of:

$$\Sigma_{vap_l}{}^{max} = \begin{cases} \frac{\min\{\gamma\rho_g, \alpha_l\rho_l\}L_h}{\Delta t_{ref} \max\{\varepsilon, |T_{sat}-T_l|\}} & \text{, if } T_{sat} < T_l \\ \frac{\gamma\alpha_g\rho_g L_h}{\Delta t_{ref} \max\{\varepsilon, |T_{sat}-T_l|\}} & \text{, if } T_{sat} \geq T_l \end{cases}, \quad \Sigma_{vap_g}{}^{max} = \begin{cases} \frac{\min\{\gamma\rho_g, \alpha_l\rho_l\}L_h}{\Delta t_{ref} \max\{\varepsilon, |T_{sat}-T_g|\}} & \text{, if } T_{sat} < T_g \\ \frac{\gamma\alpha_g\rho_g L_h}{\Delta t_{ref} \max\{\varepsilon, |T_{sat}-T_g|\}} & \text{, if } T_{sat} \geq T_g, \end{cases} \tag{29}$$

respectively, where $\varepsilon = 10^{-10}$, $\gamma = 10$ and $\Delta t_{ref} = 1$s.

4. Results

The model is used to simulate boiling in a porous medium in 2D. A uniform porosity of 0.4 (i.e. $\alpha_s = 0.4$) is assumed and the dimensions of the computational domain are 1m × 2m. The acceleration due to gravity is 9.81m/s² and gravity acts on the y direction. The material properties of the three phases are given in Table 1. The saturation temperature (in degrees Celsius) is a function of pressure (in Pa) and is calculated by:

$$T_{sat} = 500\frac{2}{\pi} \arctan\left(0.5\pi\left(p' - 5 \times 10^4\right)10^{-6}\right) - 273.15, \tag{30}$$

where:

$$p' = 1.56 \times 10^6 + C\left(p \times 10^{-5} - 10^6\right), \tag{31}$$

and:

$$C = \begin{cases} 0.5 & \text{, if } p \leq 10^{11}\text{Pa} \\ 0.3 & \text{, if } p > 10^{11}\text{Pa}. \end{cases} \tag{32}$$

Table 1. Material properties for the liquid, gas and solid phases. As far as the equations of state are concerned, the pressure is in Pa and the temperature is in degrees Celsius.

	ρ (kg/m³)	C_p (J/kg K)	κ (W/m K)	μ (Pa s)
l	$958.0966\left(1 - 2 \times 10^{-4}\left(T_l - 100\right)\right)$	4200	0.58	3×10^{-4}
g	$p/461.5(T_g+273.15)$	1996	0.016	10^{-5}
s	8000	500	16.2	0

The domain is initially saturated in water ($\alpha_l = 0.6$) and the background temperature of all three phases is 99.9°C. A perturbation in the liquid phase temperature field initial condition is used to initiate boiling. Results from three such cases with perturbation magnitude 104, 106 and 110°C are presented here. Perturbations are circular, centred around $(0.5, 0.5)$ and have a radius of 0.15m.

Free-slip boundary conditions are applied on the sides and bottom of the domain. The top boundary is assumed to be open and an atmospheric pressure condition is applied. A structured mesh of triangular elements with 20 and 40 layers in the x and y directions, respectively, is used for the three simulations.

Instantaneous maps of the vapour volume fraction at six time levels for the three simulations are shown in Fig. 1 and 2. The effect of the increased perturbation temperature on the vapourisation process is evident. For the 104 and 106°C cases the vapour starts to condense toward the end of the simulation (see Fig. 2, left and middle columns).

An additional simulation is performed using anisotropic mesh adaptivity. The model set-up is identical to the 106°C case except for the mesh. Instantaneous maps of the vapour volume fraction and vapour temperature along with the adapted mesh (bottom) at three time levels are shown in Fig. 3
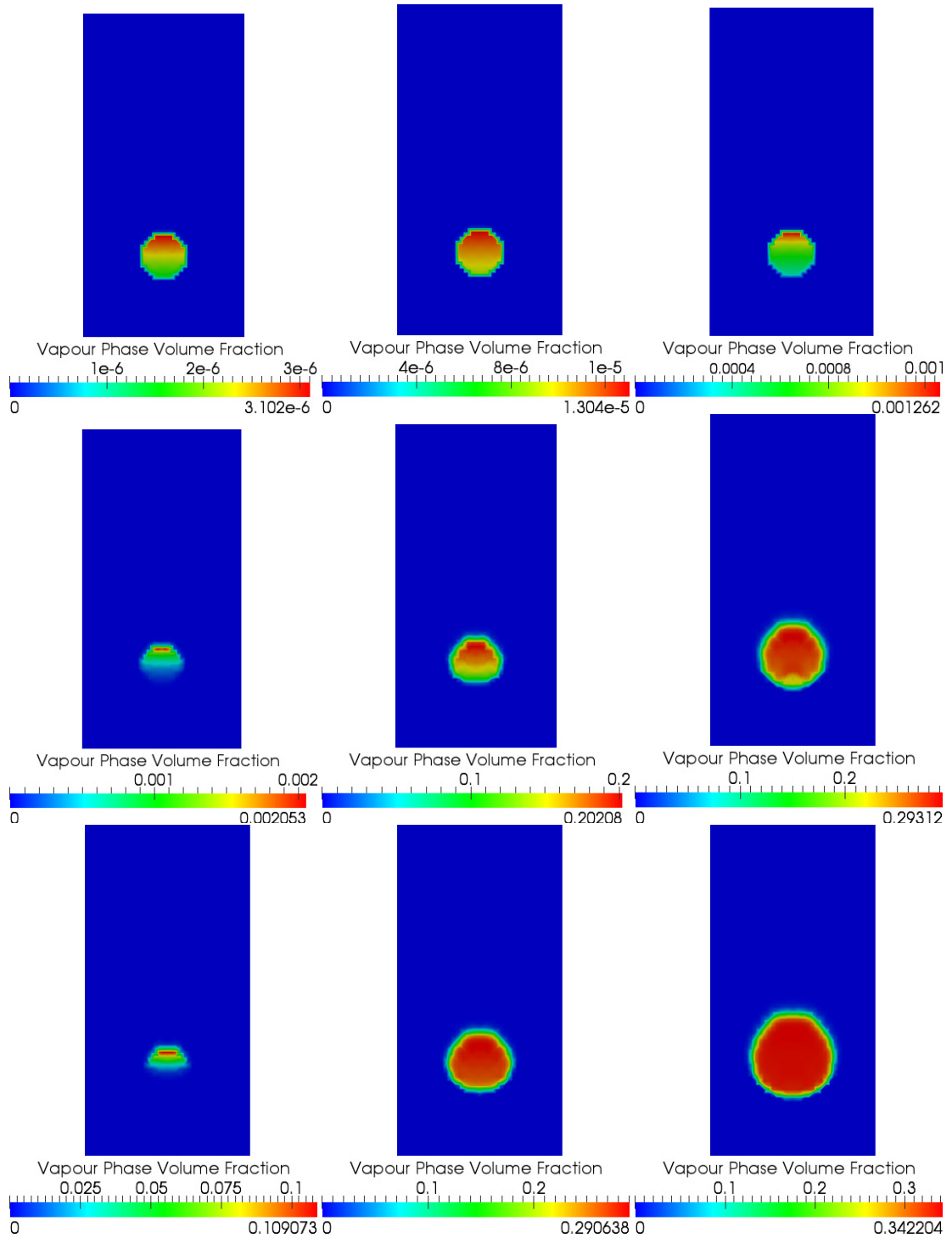
Fig. 1. Instantaneous maps of the vapour volume fraction at time levels t = 0.02, 0.4 and 0.8s from top to bottom. Left column: 104°C case. Middle column: 106°C case. Right column: 110°C case.
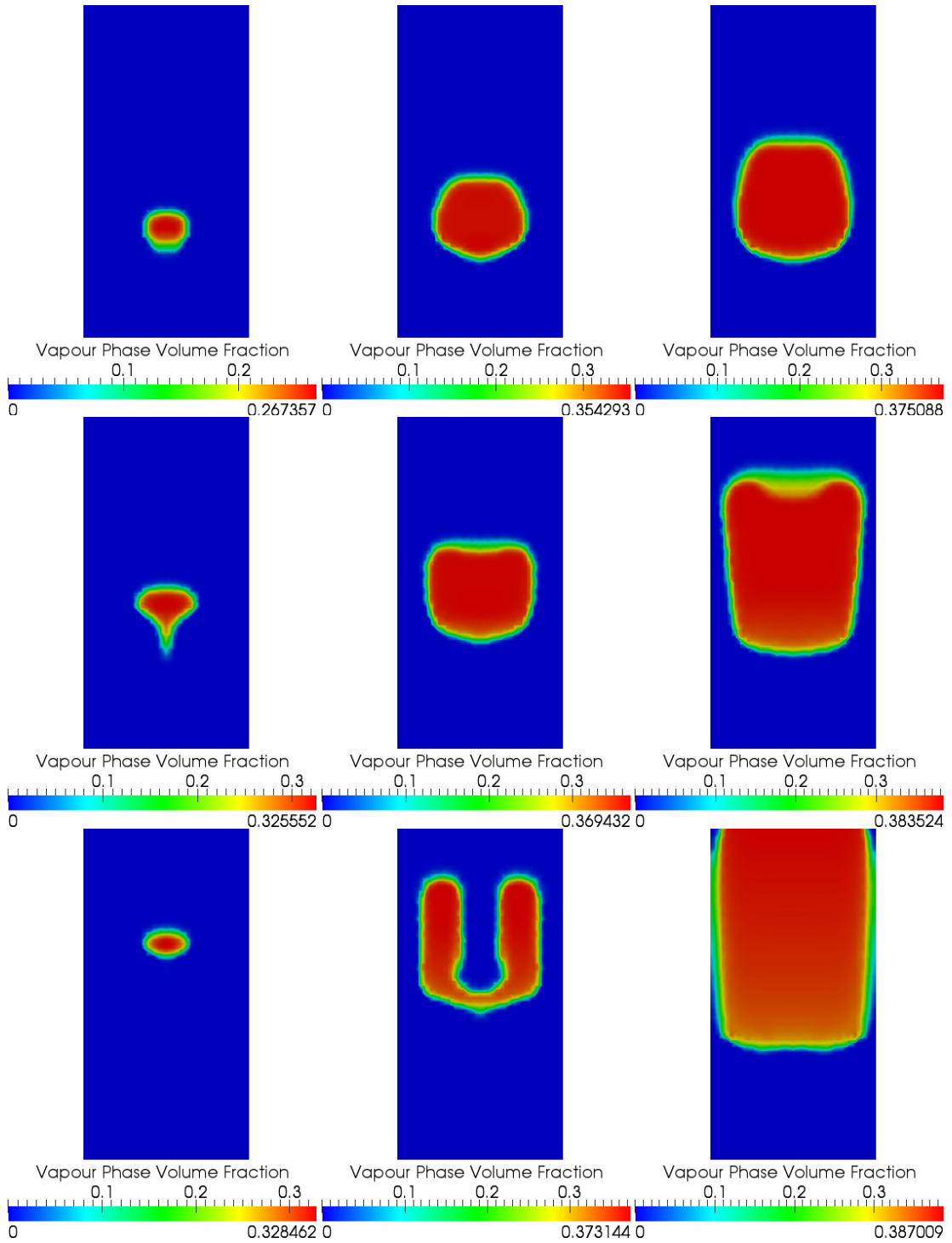
Fig. 2. Instantaneous maps of the vapour volume fraction at time levels t = 2, 4 and 8s from top to bottom. Left column: 104°C case. Middle column: 106°C case. Right column: 110°C case.
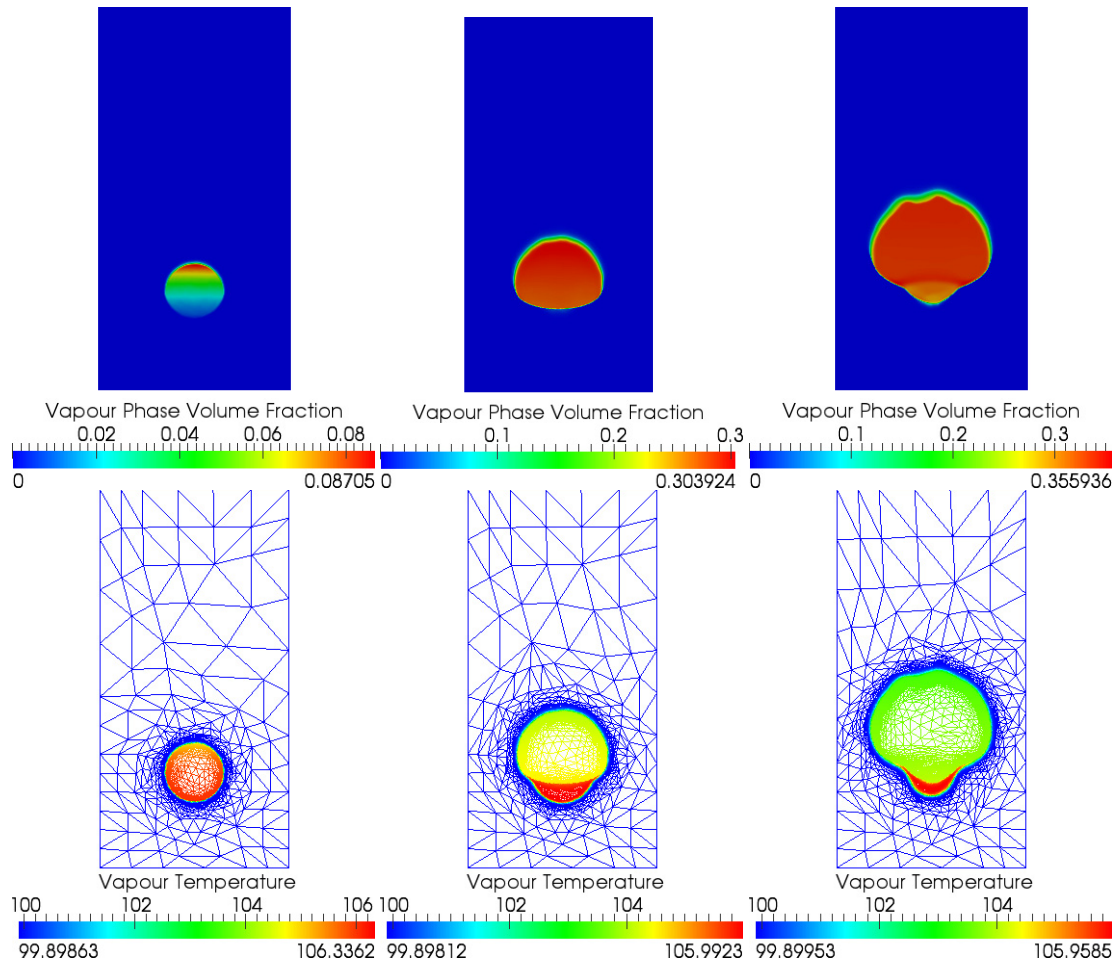
Fig. 3. Instantaneous maps of the vapour volume fraction (top) and vapour temperature along with the adapted mesh (bottom) at time levels $t = 0.2$ (left column), 1 (middle column) and 2s (right column).

5. Conclusions

A method for numerically simulating boiling in porous media has been briefly outlined here. Some features, including anisotropic mesh adaptivity, have been demonstrated through the simulations presented here.

Acknowledgements

References

1. Pain, C., de Oliveira, C., Umpleby, A.G.A.. Transient criticality in fissile solutions – compressibility effects. *Nuclear Science and Engineering* 2001;**138**:78–95.
2. Gidaspow, D.. *Multiphase flow and fluidization*. Academic Press; 1994.
3. *RELAP5-3D Code Manual Volume I: Code Structure, System Models and Solution Methods*; 2009.